Terahertz 2-D Photonic Crystal Waveguides

Adam L. Bingham and Daniel R. Grischkowsky, *Fellow, IEEE*

***Abstract*—A 2-D photonic crystal waveguide with strong passbands in the THz frequency range is demonstrated. The 2-D metallic photonic crystal waveguide structure is bounded by parallel metal plates in the vertical direction and by a square lattice of metallized cylinders on the horizontal axis. The attenuation of the photonic crystal waveguide is experimentally determined and compared to the fundamental mode of a comparably sized rectangular waveguide. The measured dispersion characteristics of the waveguide are discussed, and the output is compared to a finite-difference time-domain simulation.**

***Index Terms*—Parallel plate waveguide, photonic waveguides, quasioptic coupling, subpicosecond pulse, THz photonics.**

I. Introduction

PARALLEL plate waveguides have demonstrated excellent performance for guiding sub-ps THz pulses with little distortion on centimeter length scales [1], [2]. The parallel plate geometry has also proven useful for integrating guided-wave components [3], [4], for simulating 3-D geometries in a simpler 2-D environment [5], [6], and for the ease of coupling with free space quasi-optics. However, as THz waveguides progress towards lower loss and a higher level of device integration, some drawbacks become apparent. For example, in the unguided dimension, the beam diffracts as if in free space, leading to sizable losses for longer waveguides [2]. Additionally, the beam can only travel in one direction. While 2-D reflective [7], refractive and diffractive [8] quasi-optics have been integrated into the waveguide to control beam diffraction and direction, the optics are large, and can lead to additional losses. An alternative means of guiding within the 2-D plane, which would spatially confine the beam and provide directional control, is clearly desirable.

There has been substantial microwave work with respect to simulating, forming and demonstrating such waveguides within a larger 2-D plane, by connecting the parallel metal plates of a circuit board with arrays of metal posts which were inserted through the separating dielectric layer to form a waveguide channel [9]–[14]. It has been shown that substrate integrated waveguides (SIWs) can be formed by single rows of metal posts defining the edges of the desired waveguide channel [10], [11]. Both analysis and experiment shows the SIW has essentially the same guided wave characteristics as the corresponding conventional rectangular waveguide [10], [11]. The SIW concept has been extended (with good performance) to the situation where the edges of the guiding channel are defined by two rows of metal posts, considered as an electromagnetic bandgap (EBG) structure with a waveguide defect [12]–[14]. The EBG waveguides were formed by removing two rows of a square lattice of posts initially having six rows. EBG waveguides with four rows of posts defining the edges of the channel have been theoretically studied [14].

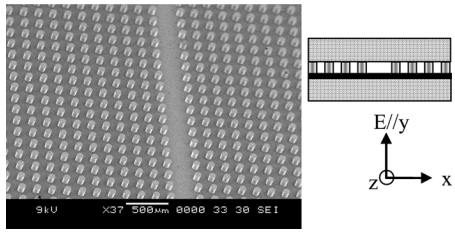

(a) (b)

Fig. 1. (a) SEM image of the PC waveguide channel. The 70 μm diameter cylinders are 70 μm tall with a period of 160 μm. The airgap is 250 μm wide at the full width of the cylinders. (b) Schematic of the entrance face of the PC waveguides with a waveguide plate on top of the cylinders.

This letter extends these ideas [9]–[14], by integrating a THz waveguide channel within a metallic 2-D photonic crystal (PC) lattice [5], bounded in the vertical dimension by a parallel plate waveguide. The geometry forms a rectangular waveguide with PC sidewalls comprised of 15 rows of metal cylinders, similar in concept to the microwave 2-D-EBG waveguide [12]–[14]. The broadband THz attenuation of the resulting PC waveguides is obtained by comparing two different lengths of waveguide. The measured output of the waveguide is compared to FDTD simulations, and the experimental attenuation is compared to the theoretical loss for a rectangular metal waveguide.

II. Fabrication and Experiment

The high-quality THz 2-D metallic photonic-crystal structures were fabricated using well developed microelectromechanical systems (MEMS) [15] and metallization technologies. First, SU-8 2025 negative photoresist from MicroChem Inc.was spun onto a 3 in Al coated Si wafer to form an 70 μm thick film. With a custom designed lithographic mask, the SU-8 film was exposed and developed. The wafer then baked at 150 °C to transform the soft SU-8 structures into permanent hard polymer structures. The channel shown in Fig. 1(a) was formed by manually removing a row of cylinders. The PC lattice was then metallized by sputtering approximately 400 nm of gold. The resulting PC waveguide chips were diced into lengths of $L_1 = 9.43$ mm (WG-1) and $L_2 = 25.4$ mm (WG-2). This procedure is easily adapted to highly precise, high-volume and relatively low-cost manufacture.

The chips were mounted into matched Al waveguides placed at the confocal beam waist of a THz TDS system. Hyper-hemispherical Si lenses were used to couple the THz beam into and

Manuscript received January 10, 2008; revised January 25, 2008. This work was supported in part by the National Science Foundation.

The authors are with the School of Electrical and Computer Engineering, Oklahoma State University, Stillwater, OK 74078 USA (e-mail: daniel.grischkowsky@okstate.edu).

Digital Object Identifier 10.1109/LMWC.2008.924906

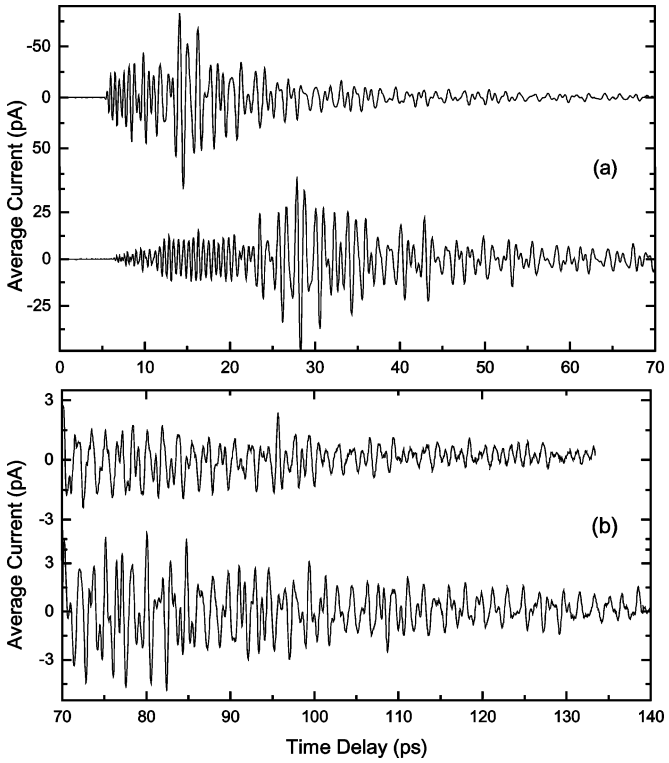

Fig. 2. (a) Average of 4 THz pulses through the $L_1 = 9.43$ mm long WG-1 (upper trace) and through the $L_2 = 25.4$ mm WG-2 (lower trace) from 0 to 70 ps. (b) THz pulse ringing of WG-1 (upper trace) and WG-2 (lower trace) from 70 to 140 ps shown on a more sensitive amplitude scale.

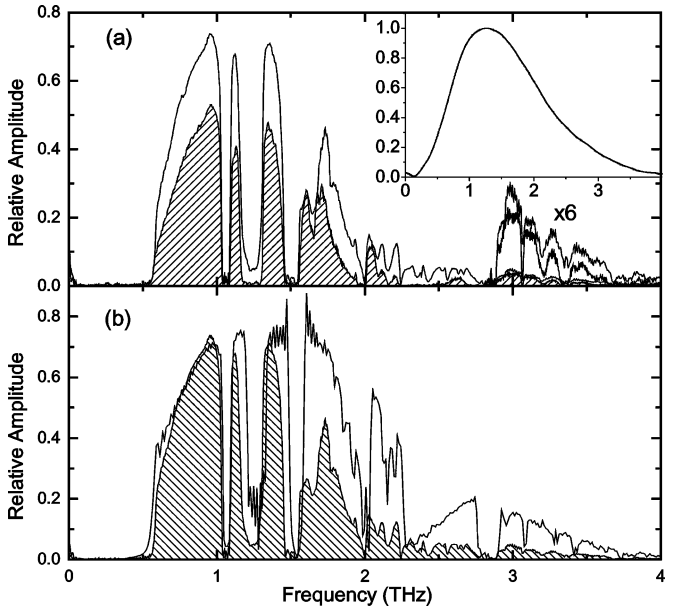

Fig. 3. (a) Normalized spectral amplitudes $E_1(\omega)$ and $E_2(\omega)$ from waveguides WG-1 and WG-2, respectively. The WG-2 spectrum is hatched for clarity. Inset: Reference spectrum without waveguide. (b) Simulated FDTD spectrum through 9.43 mm PC waveguide compared to the WG-1's measured amplitude spectrum $E_1(\omega)$ (reversed hatched).

out of the PC waveguide under test. The lenses focus a 1 THz beam to 180 μm diam. at the 250 μm $\times$70 μm waveguide aperture, shown in Fig. 1(b).

The THz pulses from WG-1 and WG-2 are shown in Fig. 2. The PC waveguides have significant dispersion resulting in the pulse ringing extending to beyond 140 ps. The high frequency content arrives first with the bulk of the lower-frequency energy coming later. The increased length of WG-2 also results in increased dispersion, as evidenced in Fig. 2(b) by the stronger ringing later in time. The Fourier-transformed amplitude spectra from the two pulses are shown in Fig. 3(a). The spectral features from the two waveguides overlap very well aside from the higher absorption in the longer waveguide, indicating the experimental reproducibility, and the excellent quality of fabrication. The transmitted bands have extremely sharp turn-ons and turn-offs of approximately 10 GHz (approaching the frequency resolution of the system) at 1.04, 1.09, 1.46, and 1.55 THz. The largest passband is approximately 0.5 THz wide between 0.6 and 1.1 THz. The remaining passbands are narrower, and the stopbands approach the noise floor. Above 2.8 THz, the spectra are also shown multiplied by a factor of 6 to better display the very sharp transmission minimum at 3.07 THz and to illustrate the noise level. The reference spectrum (normalized to unity) is inset in Fig. 3(a); it was obtained by removing the waveguide and bringing the two silicon lenses together into their confocal position, thereby maximizing the transmitted energy. For this case, the measured approximately single cycle THz pulse amplitude was 800 pA (maximum to minimum) separated by 0.27 ps. The spectra from WG-1 and WG-2 have been normalized to this reference.

As expected, the spectra show the appearance of a cutoff frequency f_c at 0.58 THz due to the rectangular waveguide provided by the PC sidewalls. For the lowest order TE_{10} mode of a rectangular waveguide, $f_c = c/2a$, where a is the width of the waveguide [16]. With $f_c = 0.58$ THz, the PC waveguide has an effective width of 258 μm rather than the 250 μm open width shown in Fig. 1(b). However, it is reasonable to expect a slightly larger effective width for the PC waveguides, due to the incomplete metal boundary. For the SIW case with single rows of cylinders defining the channel [11], and applying [11, (9)] to our case with $s = 160$ μm, $d = 70$ μm and $w = 320$ μm, we calculate $w_{\text{eff}} = 288$ μm. We believe this disagreement with our experimental result of 258 μm is due to the 15 rows of cylinders more tightly defining the channel boundary.

III. Analysis

To verify our experimental results, we performed a 2-D FDTD simulation [17] of WG-1 with perfectly conducting cylinders and using the input reference spectrum of Fig. 3(a). The experimental (reverse hatched spectrum) and theoretical output spectra are compared in Fig. 3(b). The output simulation spectrum was matched to the experimental spectrum at the peak of the first passband to illustrate the overlap. The simulation is in good agreement with the experimental results; the stopbands occur at identical locations, and the relative strengths of the passbands match well. The sharp transmission minimum observed at 3.07 THz with a FWHM linewidth of 12.4 GHz is reproduced by the simulation at 3.08 THz with similar strength and linewidth.

The measured amplitude ratio $E_2(\omega)/E_1(\omega)$ of the spectra of WG-2 to WG-1 is shown in Fig. 4(a), and in Fig. 4(b) the corresponding amplitude attenuation coefficient is compared to that calculated for the TE_{10} mode of a 70 $\times$ 258 μm rectangular

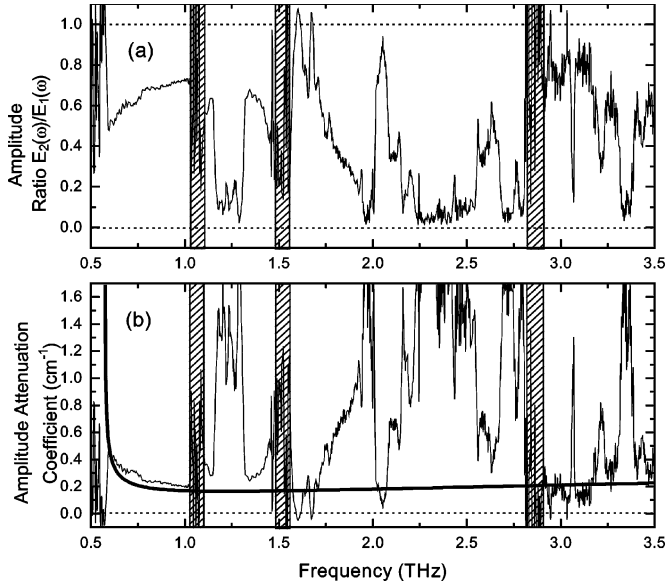

Fig. 4. (a) Amplitude ratio $E_2(\omega)/E_1(\omega)$. (b) The attenuation coefficient of the PC waveguides (upper thin line) compared to a 70×258 μm rectangular waveguide (lower thicker line). The excessively noisy stop bands are covered by hatched sections.

gold waveguide [16] (with handbook conductivity). Over most of the bandwidth, the rectangular waveguide shows less attenuation, but within the first passband of the PC waveguide the attenuations are comparable

There are four regions with acceptable S/N where the measured attenuation is less than for the rectangular waveguide. At 1.60 THz, the amplitude $E_2(\omega)$ is comparable with $E_1(\omega)$ indicating a small attenuation. However, the negative attenuation coefficient at these frequencies is considered to be due to small experimental fluctuations and noise. The 2.04 THz region has reduced absorption measured with good S/N. The broader region from 2.90 to 3.17 THz, approximately centered on the sharp absorption feature at 3.07 THz, shows a reliable measurement of reduced absorption, as shown in the 6x expanded view in Fig. 3(a). Consequently, we consider that at these indicated frequencies the measured attenuation is less than that for the rectangular waveguide.

However, absorption measurements of metallic waveguides at THz frequencies indicate a reduction of conductivity in the 100 nm THz skin-depth layer by the multiplicative factor of 1/4 [18]. For this case the rectangular waveguide attenuation shown in Fig. 4(b) would increase by the factor of 2, indicating a significant improvement in the relative loss for the 2D PC waveguides.

IV. Conclusion

The 2-D plane of the parallel plate waveguide offers an effective platform for incorporating PC waveguides. The metallic 2-D PC waveguides demonstrated here have promise to be a useful base for future THz on-chip networks, devices and instrumentation. The THz PC waveguides exhibited large pass bands with loss approaching and at certain frequencies less than that of a comparable metallic rectangular waveguide. The 2-D PC geometry is compatible with the integration of various resonators, waveguide bends and interferometers, thereby enabling new integrated components.

References

[1] R. Mendis and D. Grischkowsky, "Undistorted guided wave propagation of sub-picosecond THz pulses," *Opt. Lett.*, vol. 26, no. 11, pp. 846–848, Jun. 2001.

[2] R. Mendis and D. Grischkowsky, "THz interconnect with low loss and low group velocity dis-persion," *IEEE Microw. Wireless Compon. Lett.*, vol. 11, no. 11, pp. 444–446, Nov. 2001.

[3] A. Bingham, Y. Zhao, and D. Grischkowsky, "THz parallel plate photonic waveguides," *Appl. Phys. Lett.*, vol. 87, pp. 051101–051101, 2005.

[4] A. L. Bingham and D. Grischkowsky, "High Q, one-dimensional tera-hertz photonic waveguides," *Appl. Phys. Lett.*, vol. 90, pp. 091105–091105, 2007.

[5] Y. Zhao and D. R. Grischkowsky, "2-D THz metallic photonic crystals in parallel-plate waveguides," *IEEE Trans. Microw. Theory Tech.*, vol. 55, no. 4, pp. 656–663, Apr. 2007.

[6] Y. Zhao and D. R. Grischkowsky, "Terahertz demonstrations of effectively two dimensional photonic bandgap structures," *Opt. Lett.*, vol. 31, pp. 1534–1536, May 2006.

[7] S. Coleman and D. Grischkowsky, "A THz TEM-mode two dimensional interconnect layer incorporating quasi-optics," *Appl. Phys. Lett.*, vol. 83, no. 18, pp. 2841–2843, Nov. 2003.

[8] J. Dai, S. Coleman, and D. Grischkowsky, "Planar THz quasi-optics," *Appl. Phys. Lett.*, vol. 85, no. 6, pp. 884–886, Aug. 2004.

[9] J. Hirokawa and M. Ando, "Single-Layer feed waveguide consisting of posts for plane TEM wave excitation in parallel plates," *IEEE Trans. Antennas Propag.*, vol. 46, no. 5, pp. 625–630, May 1998.

[10] Y. Cassivi, L. Perregrini, P. Arcioni, M. Bressan, K. Wu, and G. Conciauro, "Dispersion characteristics of substrate integrated rectangular waveguide," *IEEE Microw. Wireless Compon. Lett.*, vol. 12, no. 9, pp. 333–335, Sep. 2002.

[11] F. Xu and K. Wu, "Guided-Wave and leakage characteristics of substrate integrated waveguide," *IEEE Trans. Microw. Theory Tech.*, vol. 53, no. 1, pp. 66–73, Jan. 2005.

[12] J. J. Simpson, A. Taflove, J. A. Mix, and H. Heck, "Computational and experimental study of a microwave electromagnetic bandgap structure with waveguiding defect for potential use as a bandpass wireless interconnect," *IEEE Microw. Wireless Compon. Lett.*, vol. 14, no. 7, pp. 343–345, Jul. 2004.

[13] J. J. Simpson, A. Taflove, J. A. Mix, and H. Heck, "Mode excitation from sources in 2-D EBG waveguides using the array scanning method," *IEEE Microw. Wireless Compon. Lett.*, vol. 54, no. 5, pp. 1983–1990, May 2006.

[14] F. Capolino, D. R. Jackson, and D. R. Wilton, "Mode excitation from sources in 2-D EBG waveguides using the array scanning method," *IEEE Microw. Wireless Compon. Lett.*, vol. 15, no. 2, pp. 49–51, Feb. 2005.

[15] H. Lorenz, M. Despont, N. Fahrni, N. LaBianca, P. Renaud, and P. Vettiger, "SU-8: a low-cost negative resist for MEMS," *J. Micromech. Microeng.*, vol. 7, no. 3, pp. 121–124, Mar. 1997.

[16] D. Pozar, *Microwave Engineering*. New York: Wiley, 1998.

[17] M. Qiu, "F2P: Finite-Difference Time-Domain 2D Simulator for Photonic Devices," [Online]. Available: http://www.imit.kth.se/info/FOFU/PC/F2p/

[18] N. Laman and D. Grischkowsky, "Reduced conductivity in the THz skin-depth layer of metals," *Appl. Phys. Lett.*, vol. 90, no. 12, pp. 1–3, Mar. 2007.